Searching for sharp features in the pseudogap of icosahedral quasicrystals by NMR

J. Dolinšek, M. Klanjšek, and T. Apih
J. Stefan Institute, University of Ljubljana, Jamova 39, SLO-1000 Ljubljana, Slovenia

A. Smontara
Institute of Physics, HR-10001 Zagreb, P.O. Box 304, Croatia

J. C. Lasjaunias
Centre de Recherches sur les Tres Basses Températures, CNRS, BP 166, F-38042 Grenoble Cédex 9, France

J. M. Dubois
LSG2M (UMR 7584) and GDR CINQ-CNRS, Centre d'Ingénierie des Matériaux, Ecole des Mines, Parc de Saurupt, F-54042 Nancy Cédex, France

S. J. Poon
Department of Physics, University of Virginia, Charlottesville, Virginia 22901
(Received 28 April 2000)

In a search for sharp features in the electronic density of states (DOS) of quasicrystals, a systematic comparative study of the DOS in the vicinity of Fermi energy E_F was performed in icosahedral $Al_{72.4}Pd_{20.5}Mn_{7.1}$, $Al_{62}Cu_{25.5}Fe_{12.5}$, and $Al_{70.5}Pd_{21}Re_{8.5}$ by the ^{27}Al NMR spin-lattice relaxation. The investigated samples differ markedly in their electrical conductivity (and thus the DOS at E_F) and the content of paramagnetic centers. The paramagnetism of Mn and Fe *d*-electron moments in AlPdMn and AlCuFe introduces a strong relaxation mechanism of spin diffusion to paramagnetic centers that competes with the relaxation via conduction electrons and becomes dominant at low temperatures, typically below 100 K. The $Al_{72.4}Pd_{20.5}Mn_{7.1}$ and $Al_{62}Cu_{25.5}Fe_{12.5}$ show a paraboliclike variation of the pseudogap in the DOS in the vicinity of E_F, but no sharp features were detected. In the $AlPdRe_{8.5}$ the paramagnetic relaxation is absent except at temperatures below 7 K and a single sharp feature of the full width at half height 14 meV, displaced by 11 meV from E_F, was detected. The sharp feature is very deep, reducing the DOS at the minimum to a few percent of its value in the metallic aluminum. The effect of the sharp feature in the DOS on the NMR spin lattice relaxation rate T_1^{-1} is shown theoretically to introduce a minimum in the $(T_1T)^{-1}$ product at a temperature that is crucially related to the displacement of the sharp feature from E_F.

I. INTRODUCTION

It is by now well established that the electronic density of states (DOS) in quasicrystals (QCs) exhibits a pronounced pseudogap at the Fermi energy, providing a Hume-Rothery-like electronic stabilization mechanism of the QC structure. The pseudogap was theoretically shown to be a generic property of both, the ideal QC structures[1] and their periodic approximants.[2–5] Experimentally the pseudogap was observed in many different QC and approximant samples either directly by the photoemission,[6,7] soft x-ray emission,[8,9] and tunneling and point contact spectroscopy,[10] or indirectly via the transport phenomena such as electrical conductivity and low-temperature specific heat that are compatible with an anomalously low DOS at E_F. The width of the pseudogap was found typically of the order 0.5–1 eV. There exists also an interesting theoretical prediction[1–4] that in addition to the global pseudogap at E_F, quasiperiodicity should yield a fine spiky structure of the DOS with sharp features on the energy scale of 10 meV. Such sharp features might have a profound effect on the transport properties of QCs and seem to explain the unusual behavior of the thermopower and Hall conductivity.[3] The existence of fine spiky DOS structure in the periodic approximants was demonstrated theoretically by *ab initio* calculations.[2–4] In ideal quasiperiodic structures, on the other hand, the hierarchical packing of atomic clusters shows perfect self-similarity on any spatial scale via the inflation/deflation operations, which implies that the DOS should also show a hierarchical self-similar geometry with spiky features in the pseudogap, so that the Fermi surface has a fractal character.[1] According to that ''self-similarity'' theory, the pseudogap is asymmetric and centered at E_F, showing a square root dependence of the DOS function $g(E)$ on both sides of the minimum. At temperature 0 K the semibonded electron states on the low-energy side of E_F are characterized by $g(E)=g(E_F)(1-E/E_F)^{1/2}$, whereas the free-electron band on the high-energy side obeys $g(E)\propto(E-E_F)^{1/2}$. The width of the pseudogap should essentially be zero because the inflation mechanism continuously reduces the width of the gap.[1]

From the experimental side the existence of sharp features in the DOS is still a matter of debate. Sharp features were reported in icosahedral (*i*) QCs by the NMR relaxation study,[11] whereas related NMR studies under pressure[12] found no evidence of the DOS fine structure within the 10 meV resolution. A detailed study of the DOS structure in the vi-

cinity of E_F was reported recently by the tunneling and point contact spectroscopy.[10] The tunneling experiment has observed in *i*-AlPdMn, *i*-AlCuFe, and *i*-AlPdRe a narrow, temperature-dependent anomaly in the DOS at E_F (a single sharp feature of the width of few ten meV) that develops within the broad pseudogap at low temperatures, typically below 50 K. Whereas the amplitude of the anomaly in the *i*-AlPdMn and *i*-AlCuFe was found very small, it was found significant in the *i*-AlPdRe. The anomaly effectively deepens the pseudogap at E_F and represents an additional temperature-dependent reduction of the DOS that might further improve the Hume-Rothery stabilization of the quasiperiodic structure in the limit $T \rightarrow 0$. It might also be crucially related to the low-temperature semiconductinglike and insulatinglike electronic properties of some QC families (e.g., the *i*-AlPdRe), including the reported metal-to-insulator transition.[13] The appearance of the temperature-dependent sharp feature at E_F in the DOS at low temperatures should thus have a profound effect on the electronic DOS-related physical properties of QCs.

Since the additional reduction of the DOS at E_F at low temperatures should have rather spectacular consequences for the stability and transport phenomena of the quasiperiodic structures, we undertook a systematic investigation of the pseudogap in the vicinity of E_F in high-quality *i*-$Al_{72.4}Pd_{20.5}Mn_{7.1}$, *i*-$Al_{62}Cu_{25.5}Fe_{12.5}$, and *i*-$Al_{70.5}Pd_{21}Re_{8.5}$ samples. The pseudogap was studied in the temperature interval between 300 and 4 K by the ^{27}Al NMR spin-lattice relaxation rate T_1^{-1} that depends quadratically on the DOS in the vicinity of E_F, $T_1^{-1} \propto g^2(E_F)$, and should thus be sensitive to the sharp-feature-induced reduction of $g(E_F)$. The above three samples were selected for two reasons: (i) their DOS is markedly different, the AlPdMn sample being the most (and the AlPdRe the least) conductive and (ii) the samples also have drastically different contents of the magnetic ions that can provide a parallel relaxation mechanism of spin diffusion to paramagnetic impurities and mask the effect of the sharp feature in the pseudogap. In this paper we, first give a theoretical description of the NMR spin-lattice relaxation rate in the presence of a sharp feature close to E_F within the DOS pseudogap. Then we discuss the effect of paramagnetic centers on the relaxation rate and finally compare the theory to the experiment. The presented work complements and generalizes our preliminary ^{27}Al spin-lattice relaxation study[14] on *i*-AlPdMn, which—due to the high electrical conductivity of the sample—could be explained by the two-conduction-band relaxation model.

II. THE CONDUCTION-ELECTRON RELAXATION RATE

Though being generally poor electrical conductors, QCs exhibit a finite DOS at E_F even at the lowest temperatures. The nuclear spin relaxation via conduction electrons thus represents one of the important NMR spin-lattice relaxation mechanisms in QCs. We derive here the spin-lattice relaxation rate for the coupling of the nuclear spins to the hyperfine magnetic fields of conduction electrons in the presence of a broad pseudogap and a sharp feature in the DOS that is located in the vicinity of E_F. Assuming a magnetic relaxation due to *s*-type conduction electrons as dominant, we write the relaxation rate as[15]

$$\frac{1}{T_1} = \beta_s \int dE g^2(E) f(E)[1-f(E)]. \tag{1}$$

Here the function $f(E)=\{1+\exp[(E-E_F)/k_BT]\}^{-1}$ is the Fermi-Dirac (FD) distribution. Despite the evident difference of QCs from ordinary metals, we use—in the lack of a proper theoretical description of the electronic states in quasiperiodic structures—the same proportionality constant β_s as for regular metals: $\beta_s=(64/9)\pi^3\hbar^3\gamma_e^2\gamma_n^2\langle|u_k^2(0)|\rangle_{E_F}^2$. Here γ_e and γ_n are the electron and nuclear gyromagnetic ratios and $\langle|u_k^2(0)|\rangle_{E_F}$ is the density of the electronic wave function at the nucleus averaged over the Fermi surface. We assume that $\langle|u_k^2(0)|\rangle_{E_F}$ does not exhibit sharp (energy-dependent) features. The bell-shaped FD function $f(E)[1-f(E)]=-k_BT\partial f/\partial E$ is centered at E_F and has a temperature-dependent full width at half height (FWHH) $2\Delta_f=3.5k_BT$. Since this function vanishes as E deviates from E_F by a few k_BT, it essentially selects a narrow, temperature-dependent portion of $g(E)$ around E_F, which influences the relaxation rate. At $T=300$ K $2\Delta_f$ amounts to 90 meV; whereas it decreases to 30 meV at 100 K and becomes as small as 3 meV at 10 K. The comparison of these values to the width of the pseudogap in QCs that is typically 0.5–1 eV and the expected ten meV scale of the sharp features demonstrates that the T_1^{-1} probes a narrow portion of the DOS at the very bottom of the pseudogap at E_F and—if it exists—the sharp feature.

Since the FD function $f(E)[1-f(E)]$ essentially selects a narrow portion of $g(E)$ around E_F that participates in the relaxation, the actual shape of the pseudogap is immaterial for the calculation of the relaxation rate. What matters is the curvature of $g(E)$ in the close vicinity of E_F that can always be replaced by a Taylor series expansion. We assume that the DOS in the vicinity of E_F can be described by the form

$$g(E) = g_0 + \frac{1}{2}g_0''(E-E_F)^2 - c\frac{(\Delta E_{1/2})^{\varepsilon}}{(\Delta E_{1/2})^{2\varepsilon}+|E-E_F-\delta|^{2\varepsilon}}. \tag{2}$$

The first two terms on the right side of Eq. (2) represent the parabolic Taylor series expansion of the broad pseudogap and the steepness of the parabola is given by the second derivative $g_0''=(\partial^2 g/\partial E^2)_{E_F}$. The third term represents the sharp feature located at $E_F+\delta$ (where δ accounts for the possible displacement from the exact E_F value) that is a bell-shaped function with a positive exponent $\varepsilon>0$. The sharp feature has the amplitude $c/(\Delta E_{1/2})^{\varepsilon}$ and the negative sign of c takes into account that the DOS becomes reduced because of the sharp feature. Here we assume that the third term on the right side of Eq. (2) is always smaller than the first two, so that $g(E)$ cannot become negative because of the sharp feature. For $\varepsilon=1$ the sharp feature acquires the familiar Lorentzian form, whereas for $0<\varepsilon<1$ the central part is reduced and the wings are enhanced, as compared to the Lorentzian. The quantity $\Delta E_{1/2}$ represents the half width at half height of the sharp feature that is independent of the ε value. The function $g(E)$ of Eq. (2) is displayed in Fig. 1 for several ε values. The above shape of $g(E)$ is essentially empirical, but inspired by the shapes of the differential conductance curves in the tunneling experiment[10] that are be-

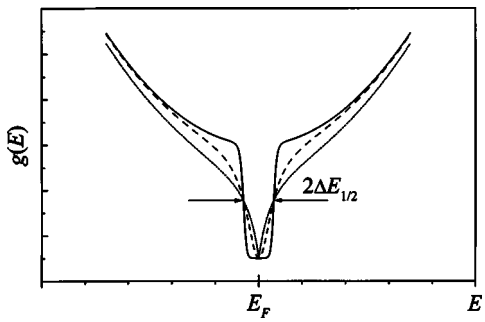

FIG. 1. Theoretical shape of the DOS function $g(E)$ in the vicinity of E_F given by Eq. (2) for several choices of the sharp-feature ''shape'' parameter ε [dotted line: $\varepsilon=0.5$; dashed line: $\varepsilon=1$ (Lorentzian); solid line: $\varepsilon=5$].

lieved to reflect closely the actual shapes of the DOS curves in the vicinity of E_F. In the absence of the sharp feature ($c=0$) the DOS at E_F is given by $g(E_F)=g_0$, whereas in its presence ($c\neq 0$) it is given by

$$g(E_F)=g_0-c\frac{(\Delta E_{1/2})^{\varepsilon}}{(\Delta E_{1/2})^{2\varepsilon}+|\delta|^{2\varepsilon}}. \tag{3}$$

The parameters of the sharp feature—the amplitude c, the width $\Delta E_{1/2}$, the ''shape'' exponent ε, and the displacement δ—may generally carry an implicit temperature-dependence.

Inserting Eq. (2) into Eq. (1) we get the conduction-electron relaxation rate T_{1c}^{-1} as

$$\begin{aligned}\frac{1}{\beta_s T_{1c}}=&g_0^2 k_B T+g_0 g_0''\frac{\pi^2}{3}(k_B T)^3\\&-2g_0 c(k_B T)^{1-\varepsilon}C(T,\Delta E_{1/2},\delta,\varepsilon)\\&+c^2(k_B T)^{1-2\varepsilon}D(T,\Delta E_{1/2},\delta,\varepsilon)\\&-g_0''c(k_B T)^{3-\varepsilon}F(T,\Delta E_{1/2},\delta,\varepsilon).\end{aligned} \tag{4}$$

The coefficients C, D, and F generally depend on the temperature and the details of the sharp feature ($\Delta E_{1/2}$, δ, and ε). Introducing new variables $x=(E-E_F)/k_B T$ and $x_\delta=\delta/k_B T$, the coefficients are defined as

$$C(T,\Delta E_{1/2},\delta,\varepsilon)=\int_{-\infty}^{\infty}dx\frac{(\Delta E_{1/2}/k_B T)^{\varepsilon}}{(\Delta E_{1/2}/k_B T)^{2\varepsilon}+|x-x_\delta|^{2\varepsilon}}\cdot\frac{e^x}{(1+e^x)^2}, \tag{5}$$

$$D(T,\Delta E_{1/2},\delta,\varepsilon)=\int_{-\infty}^{\infty}dx\frac{(\Delta E_{1/2}/k_B T)^{2\varepsilon}}{[(\Delta E_{1/2}/k_B T)^{2\varepsilon}+|x-x_\delta|^{2\varepsilon}]^2}\cdot\frac{e^x}{(1+e^x)^2}, \tag{6}$$

$$F(T,\Delta E_{1/2},\delta,\varepsilon)=\int_{-\infty}^{\infty}dx\frac{x^2(\Delta E_{1/2}/k_B T)^{\varepsilon}}{(\Delta E_{1/2}/k_B T)^{2\varepsilon}+|x-x_\delta|^{2\varepsilon}}\cdot\frac{e^x}{(1+e^x)^2}. \tag{7}$$

In the derivation of the second term on the right side of Eq. (4) the identity

$$\int_{-\infty}^{\infty}dx\,x^2\frac{e^x}{(1+e^x)^2}=\frac{\pi^2}{3}$$

was used.

In the case of no sharp feature ($c=0$), Eq. (4) yields the conduction-electron relaxation rate in the form

$$\left(\frac{1}{\beta_S T_{1c}}\right)_{\text{Korr}}=g_0^2 k_B T+g_0 g_0''\frac{\pi^2}{3}(k_B T)^3, \tag{8}$$

which can be considered as the Korringa relaxation expression for QCs (in the following referred to as the Korringa-QC relaxation) where the DOS in the vicinity of E_F is not constant ($g_0''\neq 0$), but varies parabolically due to the pseudogap.

In the presence of the sharp feature ($c\neq 0$), the relaxation rate of Eq. (4) generally depends on the temperature-dependent overlap between the FD function $f(E)[1-f(E)]$ and the sharp feature. We assume that the displacement δ of the sharp feature is small enough that the FD function (centered at E_F) and the sharp feature (centered at $E_F+\delta$) have a considerable overlap, so that their product is nonzero. If this were not so, the sharp feature would have no influence on the nuclear spin relaxation. The integrals in Eqs. (5)–(7) are determined by the area under the curve that is a product of two bell-shaped functions; the sharp feature with the FWHH $2\Delta E_{1/2}$ and the FD function with the FWHH $2\Delta_f=3.5k_B T$. The area under the product curve is determined by the narrower of the two functions.

At high temperatures the FD function is much broader than the sharp feature ($\Delta_f\gg\Delta E_{1/2}$) and we assume also that $\Delta_f\gg\delta$. The integrals C, D, and F are then determined by the area under the sharp feature curve. This can readily be seen by replacing the $e^x/(1+e^x)^2$ term in the integrals C, D, and F by $\frac{1}{4}$ in the $x\ll 1$ limit. Using a new variable $E'=E-E_F$, the integrals now become

$$C(T,\Delta E_{1/2},\varepsilon)\approx\frac{(k_B T)^{\varepsilon-1}}{4}\int_{-\infty}^{\infty}dE'\frac{(\Delta E_{1/2})^{\varepsilon}}{(\Delta E_{1/2})^{2\varepsilon}+|E'|^{2\varepsilon}}=(k_B T)^{\varepsilon-1}C_1(\Delta E_{1/2},\varepsilon), \tag{9}$$

$$D(T,\Delta E_{1/2},\varepsilon)\approx\frac{(k_B T)^{2\varepsilon-1}}{4}\int_{-\infty}^{\infty}dE'\frac{(\Delta E_{1/2})^{2\varepsilon}}{[(\Delta E_{1/2})^{2\varepsilon}+|E-E_F|^{2\varepsilon}]^2}=(k_B T)^{2\varepsilon-1}D_1(\Delta E_{1/2},\varepsilon), \tag{10}$$

and

$$F(T,\Delta E_{1/2},\varepsilon)\approx 0, \tag{11}$$

where the integrals $C_1(\Delta E_{1/2},\varepsilon)$ and $D_1(\Delta E_{1/2},\varepsilon)$ are related to the area under the sharp feature curve and the square of this curve, respectively.

The conduction-electron relaxation rate in the high-temperature limit now becomes

$$\left(\frac{1}{\beta_s T_{1c}}\right)_{\mathrm{HT}} = \left(\frac{1}{\beta_s T_{1c}}\right)_{\mathrm{Korr}} - 2g_0 c C_1(\Delta E_{1/2}, \varepsilon) + c^2 D_1(\Delta E_{1/2}, \varepsilon). \quad (12)$$

Since the Korringa-QC contribution in Eq. (12) is determined by the area under the FD function, whereas the other two terms are determined by the area under the sharp feature curve, the condition $\Delta_f \gg \Delta E_{1/2}$ implies that the Korringa-QC term is much larger than the sharp feature-dependent terms. Sharp feature in the DOS thus provides at high temperatures a small correction to the Korringa-QC relaxation law. Since the sharp-feature-dependent parameters might carry an implicit temperature dependence, the temperature dependence of the relaxation rate of Eq. (12) might exhibit a small deviation from the Korringa-QC law. Here we also note that a sharp feature on the expected energy scale of about $2\Delta E_{1/2} \approx 20\,\mathrm{meV}$ would satisfy the equality $2\Delta E_{1/2} = 3.5 k_B T$ at temperature 66 K, so that the high-temperature limit $\Delta_f \gg \Delta E_{1/2}$ is realized only at temperatures much higher than room temperature.

The temperature-dependence of the conduction-electron relaxation rate for the general case where Δ_f is comparable or smaller than $\Delta E_{1/2}$ (the situation at intermediate and low temperatures) and in addition $\delta \neq 0$ (the sharp feature is displaced from E_F), is more complicated. The relaxation rate is now given by the full Eq. (4) and its temperature dependence is best discussed via the original formula of Eq. (1). For a simple illustration we assume first a constant $g(E)$ (as in ordinary metals) and consider the effect of the sharp feature on the relaxation rate. This consideration is easily generalized to the case of parabolic $g(E)$. For a constant $g(E)$ the area under the FD curve is directly proportional to $k_B T$ and this is the only source of temperature dependence in the integral of Eq. (1) Consider now the presence of a sharp feature that is displaced from E_F by δ. For simplicity we assume that the shape of the sharp feature does not depend on temperature. At not too low temperatures the FD function will still be broad enough to integrate over the sharp feature in Eq. (1). However, due to the reduced DOS within the sharp feature, the integral is reduced as compared to $g(E)$ of the no-sharp-feature case. On lowering the temperature, the FD function narrows to the extent that the integration is no more performed over the displaced sharp feature and the integral again equals that of the $g(E) = \mathrm{const}$ case, following again the $k_B T$ dependence. The above behavior is best observed in the $(T_{1c}T)^{-1}$ vs T scale, which eliminates the linear $k_B T$ dependence and shows only the departure from it. At high temperatures the FD function is broad and the integral of Eq. (1) is performed over a large portion of $g(E)$, so that—as stated above—the sharp feature has effectively no influence. On lowering the temperature, the FD function narrows continuously and the influence of the sharp feature becomes gradually more important. Its main effect is to decrease the $(T_{1c}T)^{-1}$ product below the value of the no-sharp feature case. At still lower temperatures the displaced sharp feature no more participates in the integration, so that the $(T_{1c}T)^{-1}$ product increases again. The existence of the displaced sharp feature in the DOS thus results in a formation of a minimum in the product $(T_{1c}T)^{-1}$ at a temperature that depends on the displacement δ. The minimum occurs roughly at a temperature where the width of the FD function

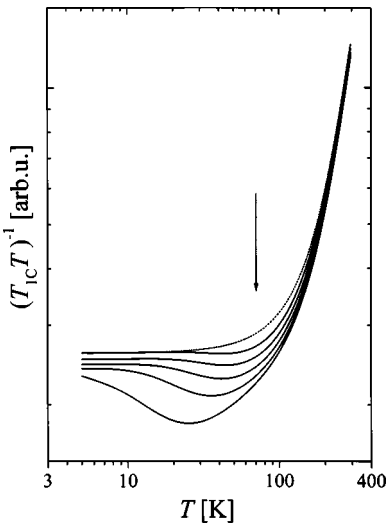

FIG. 2. Theoretical temperature dependence of the conduction-electron relaxation rate product $(T_{1c}T)^{-1}$ calculated from Eq. (4) for the case that a sharp feature close to E_F is present in the DOS. Solid lines are $(T_{1c}T)^{-1}$ curves calculated for several values of the displacement parameter δ (from top to bottom at the position of the arrow: $\delta = 12,10,8,6,4$ meV). The dashed line represents the no-sharp feature case that obeys the Korringa-QC form of the type $(T_{1c}T)^{-1} = a + bT^2$. The parameters used in the calculation are $g_0''/g_0 = 760\,(\mathrm{eV})^{-2}$, $c/[g_0(\Delta E_{1/2})^{\varepsilon}] = 0.9$, $\Delta E_{1/2} = 2$ meV, $\varepsilon = 5$, and $g_0 = 0.165$ [g_0 is here dimensionless and should be considered as normalized to the value of the metallic aluminum, i.e., $g_0/g_0(\mathrm{Al})$].

Δ_f and the displacement δ of the sharp feature from E_F are equal. Clearly, the larger the displacement, the higher the temperature of the minimum. In Fig. 2 we show theoretically [using Eq. (4)] the occurrence of the sharp-feature-induced minimum in the temperature dependence of the $(T_{1c}T)^{-1}$ product. The curves in Fig. 2 are calculated for different displacement parameters δ, showing two general trends: (i) a smaller δ creates the minimum at lower temperatures and (ii) the closer the sharp feature to the E_F, the larger its effect (the deeper the minimum). Relaxing now the assumption of a temperature-independent sharp feature, we note that its possible temperature-dependence shall affect the depth, the width and the position of the minimum in the temperature-dependent $(T_{1c}T)^{-1}$ curves. Finally we note that despite the large number of parameters used to describe the sharp feature in our model $(c, \Delta E_{1/2}, \varepsilon, \delta)$, only two quantities are physically relevant; (i) the area of the sharp feature (determined by the combination of the parameters $c, \Delta E_{1/2}, \varepsilon$) and (ii) its displacement δ from E_F. For that reason the particular c, $\Delta E_{1/2}$ and ε values obtained from the fit procedure should be considered as qualitative only.

III. RELAXATION VIA PARAMAGNETIC CENTERS

An important nuclear spin relaxation mechanism in QCs can also be the relaxation via paramagnetic centers (such as Mn or Fe *d*-electron moments) in combination with spin diffusion. It is well known that paramagnetic impurities even in *ppm* concentrations can bypass all the other relaxation mechanisms. In many QCs the concentration of paramagnetic centers is very high. In *i*-AlPdMn a fraction of about

1% of all the manganese atoms carries large *d*-electron magnetic moments with magnitudes close to five Bohr magnetons.[16,17] In *i*-AlCuFe a fraction 10^{-4} of the total number of Fe atoms are magnetic.[10,18] Due to these high concentrations it would be very unlikely not to observe the paramagnetic relaxation in the spin-lattice relaxation experiments. It is therefore rather unusual that the relaxation via paramagnetic centers was not reported so far in the NMR relaxation studies of QCs.

For simplicity we consider the paramagnetic centers in QCs as localized. The relaxation of nuclear spins via the magnetic dipole-dipole coupling to the paramagnetic electrons in combination with spin diffusion between spatially remote resonant nuclei was treated by Abragam.[19] The relaxation rate was found to be

$$\frac{1}{T_{1P}} = 4\pi N \kappa D, \tag{13}$$

where N is the concentration of paramagnetic centers in the sample with the average separation between the centers $R = N^{-1/3}$ and D is the diffusion constant for the nuclear spin magnetization transfer in space. D is of the order Wa_0^2, where a_0 is the nearest-neighbor distance and W is the probability rate of a spin flip-flop transition between nearest neighbors (induced by the flip-flop term of the magnetic dipole-dipole interaction between nuclear spins). The coefficient κ depends on whether the electronic fluctuations are slow or fast with respect to the nuclear Larmor frequency $\omega_0 = \gamma_n H_0$ (with H_0 being the external magnetic field). Defining τ as the longitudinal electron relaxation time,[19] we get in the slow-motion limit $\omega_0 \tau \gg 1$

$$\kappa \approx a_0 \left(\frac{H_e^0}{H_0} \right)^{1/2} (W\tau)^{-1/4}, \tag{14}$$

where $H_e^0 = \gamma_e \hbar / a_0^3$ is the electronic local field at a distance a_0 from the paramagnetic electron. The relaxation rate in this limit depends on the external magnetic field and τ as $T_{1P}^{-1} \propto H_0^{-1/2} \tau^{-1/4}$.

In the fast motion limit $\omega_0 \tau \ll 1$ we get, on the other hand,

$$\kappa \approx \gamma_n^{1/2} a_0 (H_e^0)^{1/2} \left(\frac{\tau}{W} \right)^{1/4}, \tag{15}$$

so that $T_{1P}^{-1} \propto \tau^{1/4}$ and is field independent. The electron relaxation time τ is usually in the fast motion limit with respect to the nuclear Larmor frequency. In diluted paramagnets, where the interaction between the electronic moments is negligible, τ normally does not exhibit pronounced temperature dependence, so that the paramagnetic relaxation rate of Eq. (13) is to a good approximation temperature-independent. In metallic systems with correlated electrons the electronic fluctuations in many cases exhibit a slowing-down dynamics at low temperatures, the most common cases involving critical phenomena preceding a cooperative magnetic phase transition or the onset of spin-freezing in spin-glass systems. In such a case T_{1P}^{-1} shall exhibit a temperature-dependent increase on cooling proportional to $\tau^{0.25}$ (or better as τ^m with m slightly different from 0.25 due to the effect of electronic correlations) that shall follow the increase of τ at low temperatures.

IV. EXPERIMENTAL

The ^{27}Al NMR spin-lattice relaxation experiment was performed on three high-quality icosahedral samples: i-$Al_{72.4}Pd_{20.5}Mn_{7.1}$, i-$Al_{62}Cu_{25.5}Fe_{12.5}$, and i-$Al_{70.5}Pd_{21}Re_{8.5}$. The i-$Al_{72.4}Pd_{20.5}Mn_{7.1}$ (referred to as $AlPdMn_{7.1}$) was a monodomain sample used before in NMR diffusion[20] and relaxation[14] studies. Magnetic susceptibility measurements in the temperature interval 300–20 K detected a fraction 1% of the total number of Mn atoms to be magnetic, in agreement with the results on similar concentrations.[16,17] The i-$Al_{62}Cu_{25.5}Fe_{12.5}$ ($AlCuFe_{12.5}$) was a polygrain sample, used before in a specific-heat study.[18] Its composition corresponds to the perfect icosahedral structure, stable at every temperature, and the high structural quality of the sample was demonstrated by the lack of broadening of the x-ray diffraction peaks at their base. Magnetic investigations estimated a fraction 1.5×10^{-4} of the total number of Fe atoms to be magnetic (spin $S=2$). The i-$Al_{70.5}Pd_{21}Re_{8.5}$ ($AlPdRe_{8.5}$) was also a polygrain sample, its high quality being demonstrated by the large room-temperature electrical resistivity $\rho_{300\,K} = 16000\,\mu\Omega$cm and the resistivity ratio $\rho_{4\,K}/\rho_{300\,K} = 114$. This sample is considered to be perfectly diamagnetic, the estimated level of magnetic impurities being less than a *ppm*. Magnetic susceptibility measurements on a similar composition $Al_{70}Pd_{21.4}Re_{8.6}$ detected[21] a small Curie upturn at temperatures below 10 K that was attributed to the usual impurity contamination of a nominally pure diamagnetic sample. The three samples thus differ markedly in the concentration of the paramagnetic centers. The electrical conductivity of the samples that is directly related to the magnitude of the electronic DOS at E_F is also different, with the $AlPdMn_{7.1}$ being the most and the $AlPdRe_{8.5}$ the least conductive. Our choice of the samples thus enabled us to perform a systematic comparative study of the DOS in the vicinity of E_F in the samples with different electrical conductivity and concentration of paramagnetic centers.

V. RESULTS AND DISCUSSION

The ^{27}AlNMR spin-lattice relaxation experiments were performed in the temperature interval from 300 to 4 K at the resonance frequency $\nu_0(^{27}\mathrm{Al}) = 26.134$ MHz. The saturation-recovery pulse sequence was used with a saturation train of sixty $\pi/2$ pulses of 2 μ sec duration. The spin-lattice relaxation rate T_1^{-1} was extracted from the magnetization-recovery curves by the long-saturation magnetic relaxation model, as described in Ref. 14. The use of this model assumes that the dominant relaxation in the investigated QCs is of magnetic origin and considers the possible electric quadrupole relaxation contribution as less important.

The ^{27}Al T_1^{-1} data of all three investigated samples show qualitatively similar decreasing behavior on cooling from room temperature to 4 K [Fig. 3(a)]. The decrease is, however, not monotonous, but exhibits interesting features in different temperature intervals that are best observed in the $(T_1T)^{-1}$ vs T plot [Fig. 3(b)]. A true Korringa-metallic-type relaxation via *s*-conduction electrons would yield a straight

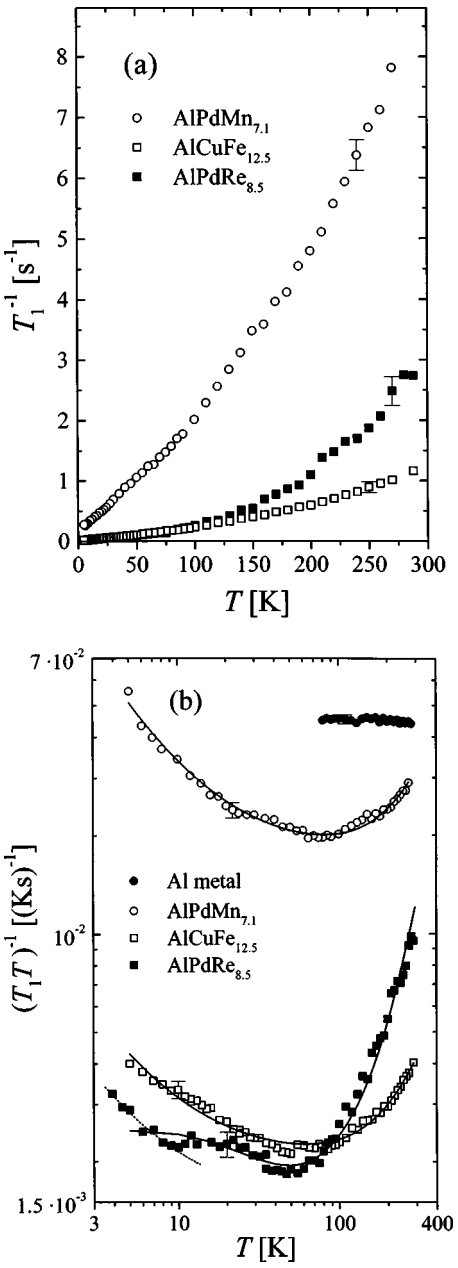

FIG. 3. (a) ^{27}Al T_1^{-1} data of the $AlPdMn_{7.1}$, $AlCuFe_{12.5}$, and $AlPdRe_{8.5}$ samples in the temperature interval from room temperature to 4 K. (b) Same data as in (a) displayed in the $(T_1T)^{-1}$ vs T plot. The data of the metallic aluminum are shown for comparison. Solid lines are theoretical fits discussed in the text. Dashed line is the estimated paramagnetic relaxation contribution below 7 K in the $AlPdRe_{8.5}$.

horizontal line ($T_1T=$const) in this plot, whereas the ^{27}Al $(T_1T)^{-1}$ experimental data show a pronounced difference to the Korringa-metallic prediction. The $(T_1T)^{-1}$ values first decrease from room temperature in a paraboliclike T^2 manner and exhibit a minimum somewhere below 100 K. In the $AlPdMn_{7.1}$ the minimum occurs at $T\approx 100$ K, whereas the minimum is shifted to 80 K in the $AlCuFe_{12.5}$ and to 50 K in the $AlPdRe_{8.5}$. Below the minimum the trend is reversed and $(T_1T)^{-1}$ starts to increase on further cooling down to the lowest measured temperature of 4 K. The quadraticlike behavior of $(T_1T)^{-1}$ on the high-temperature side of the minimum was already observed in QCs before,[11,14,22] and its origin was attributed to the variation of the DOS function $g(E)$ in the vicinity of E_F. The low-temperature $(T_1T)^{-1}$ increase on cooling, though also reported previously,[22] remains still an open problem. The investigated QCs thus show a temperature dependence of T_1^{-1} that is drastically different from that of ordinary metals, despite their evident residual metallic character. In Fig. 3(b) the ^{27}Al $(T_1T)^{-1}$ data of metallic aluminum in the temperature interval from room temperature to 77 K are displayed for comparison. The data obey the Korringa-metallic relation $(T_1T)^{-1}=\beta_s k_B g_0^2=4.6\times 10^{-2}\,\mathrm{s^{-1}\,K^{-1}}$.

The peculiar temperature dependence of the relaxation rates displayed in Fig. 3(b) can be explained by considering the ^{27}Al relaxation rate to be a sum of two relaxation mechanisms—the relaxation via the conduction electrons and the relaxation via the paramagnetic centers: $T_1^{-1}=T_{1c}^{-1}+T_{1P}^{-1}$. The conduction-electron contribution is taken in the form of Eq. (4) whereas the paramagnetic relaxation in combination with spin diffusion is taken in the form of Eq. (13). We consider the electronic fluctuations to be in the fast motion limit with respect to the nuclear Larmor frequency, which is supported by the observed field-independence of the ^{27}Al relaxation rate[14] in $AlPdMn_{7.1}$ below 100 K. The parameter κ is then given by the Eq. (15) and we can write T_{1P}^{-1} abbreviated as $T_{1P}^{-1}=\Gamma\tau^{1/4}$. Here the constant Γ is considered to be temperature-independent. In the following we discuss the three samples separately.

A. $AlPdMn_{7.1}$

The $AlPdMn_{7.1}$ is the most conductive of the three investigated samples and hence has the largest DOS at E_F. In addition, it contains the largest number of paramagnetic centers. As a consequence, the relaxation contributions T_{1c}^{-1} and T_{1p}^{-1} are both stronger than in the $AlCuFe_{12.5}$ and $AlPdRe_{8.5}$, so that $AlPdMn_{7.1}$ exhibits the largest total ^{27}Al relaxation rate [Fig. 3(b)]. The $(T_1T)^{-1}$ data can be well reproduced by the formula

$$\frac{1}{T_1T}=a+bT^2+\frac{d}{T}, \tag{16}$$

with $a=\beta_s k_B g_0^2$, $b=\beta_s g_0 g_0''(\pi^2/3)k_B^3$, and $d=\Gamma\tau^{1/4}$ that is valid in the absence of the sharp feature in the DOS. The fit procedure yielded the parameter values $a=(1.7\pm 0.1)\times 10^{-2}\,\mathrm{s^{-1}\,K^{-1}}$, $b=(1.58\pm 0.1)\times 10^{-7}\,\mathrm{s^{-1}\,K^{-3}}$, and $d=(0.17\pm 0.004)\,\mathrm{s^{-1}}$. From the parameter a we may estimate the reduction of the DOS in the $AlPdMn_{7.1}$ with respect to the metallic aluminum but the calculation is hampered by the fact that the electronic wave function density $\langle|u_k^2(0)|\rangle_{E_F}$ at the ^{27}Al nuclei that appears in β_s is not known neither for the $AlPdMn_{7.1}$ nor for the other two investigated QCs. So we can only speculate that it does not change much as compared to the metallic aluminum. Using this assumption we find the ratio $g_0/g_0(\mathrm{Al})=0.61$, which gives the reduction of the DOS at E_F in the $AlPdMn_{7.1}$ by a factor 1.64 with respect to the Al metal. From the parameters a and b we also determine the ratio $g_0''/g_0=3b/(a\pi^2k_B^2)$, which for $AlPdMn_{7.1}$ amounts to 384 $(\mathrm{eV})^{-2}$.

The growth of the $(T_1T)^{-1}$ below the minimum at 100 K can be well reproduced by the paramagnetic term d/T with a temperature-independent parameter d. This temperature independence demonstrates that the paramagnetic relaxation mechanism in the investigated temperature range between 100 and 4 K is most likely the simple ^{27}Al spin diffusion to paramagnetic Mn centers. The analogy to the *i*-AlPdMn samples containing about 9% of Mn, which undergo a transition to a spin glass state [i.e., at $T_g \approx 1.1$ K in $Al_{68.7}Pd_{21.7}Mn_{9.6}$ (Ref. 23) and 0.5 K in $Al_{70}Pd_{21}Mn_9$ (Ref. 17)] indicates that in the $AlPdMn_{7.1}$ one may also expect at low temperatures a stronger increase of the paramagnetic relaxation rate due to the slowing-down of the electronic fluctuations. No such increase was detected in our experiment down to the lowest measured temperature of 4 K, but a precise systematic study of this effect was also not performed.

The increase of the $(T_1T)^{-1}$ on cooling cannot be explained in an alternative way by the conduction-electron relaxation mechanism, for which the data should saturate at low temperature to a constant plateau, the value of which should be considerably smaller than the $(T_1T)^{-1}$ value at room temperature. In Fig. 3(b) it is seen that the $(T_1T)^{-1}$ values at 4 K are a factor of 2 larger than at 290 K, and, moreover, below 10 K they even become larger than those of the metallic aluminum. This excludes the possible dominance of the conduction-electron relaxation at low temperatures. The minimum at 100 K is thus a result of the crossover from the dominant conduction-electron relaxation at high temperatures to the dominant paramagnetic relaxation at low temperatures.

The overall temperature dependence of the $(T_1T)^{-1}$ data can thus be well reproduced by the Eq. (16), which assumes the absence of the sharp feature in the DOS. This should not, however, be taken as the ultimate proof for the nonexistence of the sharp feature in the $AlPdMn_{7.1}$. The amplitude of the sharp feature may either be too small to be detected or its effect may occur at such temperatures where it is masked by the dominant paramagnetic relaxation.

B. $AlCuFe_{12.5}$

The temperature dependence of the ^{27}Al $(T_1T)^{-1}$ in the $AlCuFe_{12.5}$ is qualitatively similar to that of the $AlPdMn_{7.1}$, but significant quantitative differences exist. The differences result from (i) the smaller conductivity of the $AlCuFe_{12.5}$ (smaller DOS at E_F) and (ii) the smaller fraction of paramagnetic centers by two orders of magnitude. As a result, the two relaxation contributions T_{1c}^{-1} and T_{1P}^{-1} are both smaller than in the $AlPdMn_{7.1}$. This is observed in Fig. 3(b), where the product $(T_1T)^{-1}$ of the $AlCuFe_{12.5}$ exhibits about five-time smaller magnitude from that of the $AlPdMn_{7.1}$ in the whole investigated temperature range. The data could be again well reproduced by Eq. (16), which assumes the absence of the sharp feature in the DOS. The fit parameters values $a=(2.0\pm0.05)\times10^{-3}\,s^{-1}K^{-1}$, $b=(2.4\pm0.1)\times10^{-8}\,s^{-1}K^{-3}$, and $d=(1.1\pm0.04)\times10^{-2}\,s^{-1}$ yield the ratio $g_0''/g_0=490\,(eV)^{-2}$ and $g_0/g_0(Al)=0.21$, which gives the reduction of the DOS at E_F in the $AlCuFe_{12.5}$ by a factor 4.8 with respect to the Al metal.

The increase of the $(T_1T)^{-1}$ below the minimum at about 80 K is again consistent with the dominant relaxation by the temperature-independent spin diffusion to paramagnetic Fe moments. The paramagnetic constant d in the $AlCuFe_{12.5}$ is by a factor 15 smaller than in the $AlPdMn_{7.1}$ that is in qualitative agreement with the smaller number of moments.

C. $AlPdRe_{8.5}$

The ^{27}Al nuclear spin relaxation in the $AlPdRe_{8.5}$ is a special case that shows qualitatively different features from the $AlPdMn_{7.1}$ and $AlCuFe_{12.5}$ compounds. One of the reasons is the diamagnetic character of the sample with the level of paramagnetic impurities being of the order of a *ppm* or less. The strong paramagnetic relaxation is thus absent in the $AlPdRe_{8.5}$, except at temperatures close to $T\rightarrow0$. The possible existence of the sharp feature in the DOS in the vicinity of E_F shall thus not be masked by the paramagnetic relaxation. On the other hand, the electrical conductivity of the $AlPdRe_{8.5}$ is the smallest of all the investigated samples, so one can expect that the pseudogap in the vicinity of E_F shall be the deepest and the steepest.

The above considerations are indeed observed in Fig. 3(b). The high-temperature T^2 decrease of the $(T_1T)^{-1}$ data is the strongest of all the investigated samples, demonstrating the largest second derivative g_0'' and hence the steepest pseudogap. At the temperature 50 K a shallow minimum is observed that is followed by a slight increase and then leveling-off of the $(T_1T)^{-1}$ data to a temperature-independent value down to 7 K. This kind of behavior was shown in Sec. II. to result from the existence of a sharp feature in the DOS that is slightly displaced from the exact E_F value. The subsequent slight increase of $(T_1T)^{-1}$ below 7 K results from the paramagnetic relaxation due to the small residual fraction of the extrinsic magnetic moments that starts to dominate over the conduction-electron relaxation mechanism on approaching $T\rightarrow0$.

The $(T_1T)^{-1}$ data in the interval from room temperature down to 7 K could be well reproduced by the Eq. (4) that takes into account the presence of the sharp feature in the DOS. The fit yielded the broad pseudogap parameters $a=(1.75\pm0.5)\times10^{-3}\,s^{-1}K^{-1}$ and $b=(9.8\pm0.5)\times10^{-8}\,s^{-1}K^{-3}$ that give $g_0''/g_0=2.3\times10^3\,(eV)^{-2}$ and $g_0/g_0(Al)=0.19$. Comparing the g_0'' value to the other two investigated QCs we find that the broad pseudogap is indeed the steepest in the $AlPdRe_{8.5}$.

The interesting result is the discovery of the sharp feature in the pseudogap that is slightly displaced from E_F. The fit procedure yielded the displacement $\delta=11$ meV. The other three parameters that determine the shape of the sharp feature were obtained as follows: the ''shape'' exponent $\varepsilon=5$, the FWHH $2\Delta E_{1/2}=14$ meV and the amplitude normalized to g_0 as $c/\{g_0(\Delta E_{1/2})^{\varepsilon}\}=0.9$. A satisfactory fit could be made by taking all the above parameters as temperature independent. The precision of the experiment, however, does not allow us to be more specific about their possible temperature dependence and also does not exclude their weak temperature dependence. As already discussed, the parameters c, ε, and $\Delta E_{1/2}$ slightly compensate each other in the fit procedure. The resulting shape of the sharp feature should thus be considered qualitatively only, the relevant parameter being the area under the sharp feature curve. The displacement δ, on the other hand, determines the temperature of the

minimum in the $(T_1T)^{-1}$ and interferes only insignificantly with the other parameters, so that its value can be considered also quantitatively. The fact that the minimum in the DOS is displaced from E_F (due to the displaced sharp feature) may not be too surprising in view of the Hume-Rothery stabilization mechanism in QCs. A Hume-Rothery alloy with a given electron concentration (average number of valence electrons per atom) builds up the structure in such a way that the resulting Brillouin zone boundary induces a pseudogap in the DOS at the Fermi level. The exact position of the pseudogap minimum with respect to the E_F is determined by the average number of valence electrons per atom that depends on the actual concentration of the incoming compounds in the alloy. Only for a rather sharp concentration ratio (that leads to an ''ideal'' icosahedral composition) the minimum of the pseudogap and the E_F shall coincide, whereas for a slight mismatch of the composition, the pseudogap shall generally be displaced from E_F. The existence of the sharp ''ideal'' composition, which is the only one that gives a true long-time (thermodynamics) structural stability, is well known for icosahedral QCs, so that the mismatch between the pseudogap minimum and the E_F due to the nonideality of the composition in real QC samples should be observed more as a rule than as an exception. The observed displacement of the DOS minimum from the E_F in the $AlPdRe_{8.5}$ sample can thus be attributed to the small deviation from the ideal icosahedral composition. On the other hand, the small magnitude of the displacement of 11 meV demonstrates that its composition is in reality not far from ideal.

The small ''Curie upturn'' in the $(T_1T)^{-1}$ below 7 K can be attributed to the residual paramagnetic relaxation. The available data points allow only an estimate of the parameter $d \approx 6\times10^{-3}\,s^{-1}$ that is one order of magnitude smaller compared to the $AlCuFe_{12.5}$, in agreement with the reduced number of paramagnetic centers in the $AlPdRe_{8.5}$.

The above analysis enables us to make a qualitative reconstruction of the DOS in the vicinity of E_F for all three investigated QCs using their respective g_0 and g_0'' values as well as the parameters of the sharp feature for the $AlPdRe_{8.5}$. A true quantitative reconstruction is not possible due to the fact that the NMR determination of the g_0 and g_0'' parameters relies on the assumption that the electronic wave function density $\langle|u_k^2(0)|\rangle_{E_F}$ at the ^{27}Al nuclei in the investigated QCs is the same as in the metallic aluminum. In view of the evident difference between the extended electronic states in ordinary metals and the critical states in QCs, this assumption cannot be justified in a simple way. The NMR-reconstructed DOS functions of the $AlPdMn_{7.1}$, $AlCuFe_{12.5}$ and $AlPdRe_{8.5}$ normalized to the DOS of the metallic aluminum are displayed in Fig. 4. The pseudogap in the $AlPdMn_{7.1}$ is shallow and its value at E_F is relatively large, amounting to 60% of the DOS of the metallic aluminum. Hence the $AlPdMn_{7.1}$ has a rather strong metallic character. The pseudogap in the $AlCuFe_{12.5}$ is much deeper, reaching at E_F about 20% of the Al metal DOS. The $AlPdRe_{8.5}$ has the deepest and the steepest pseudogap and exhibits the sharp feature displaced by 11 meV from the E_F. The sharp feature has large amplitude and reduces the DOS at the minimum to a few percent of the Al metal DOS only. This is consistent with the very high electrical resistivity of the AlPdRe sample

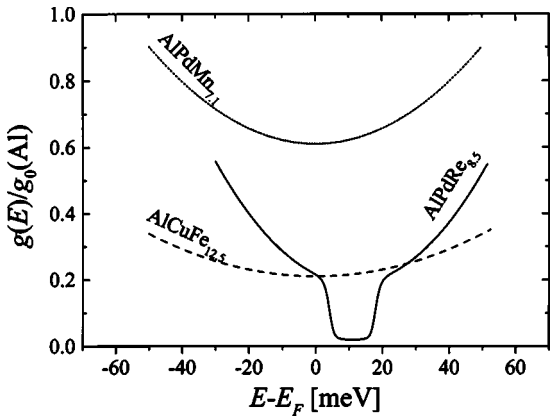

FIG. 4. The DOS functions in the vicinity of E_F of the investigated $AlPdMn_{7.1}$, $AlCuFe_{12.5}$, and $AlPdRe_{8.5}$ samples reconstructed from their respective g_0, g_0'' and the sharp feature parameter values obtained from the $(T_1T)^{-1}$ fits.

and the observed metal-to-insulator transition at low temperature in this family. On the other hand, it raises a question whether in this case one is still allowed to distinguish between the broad pseudogap and the sharp feature, or one is in reality dealing with a unique global shape of the pseudogap that exhibits a deep and narrow valley in the close vicinity of E_F and becomes broader paraboliclike at larger distances. Another problem is the comparison of the energy scales of the pseudogaps determined by NMR as shown in Fig. 4 and the tunneling experiment,[10] where the NMR-determined pseudogaps are by a factor 2–3 narrower than those of the tunneling experiment. This inconsistency very likely originates from the use of the NMR relaxation model of Eq. (1) that is derived for the conduction electrons in the form of extended Bloch waves instead of the QC-specific critical states that are not extended but localized over many interatomic distances. To derive a better spin-lattice relaxation model for QCs in the presence of such electrons is at present a difficult task due to the lack of a proper theoretical description of critical states. One is thus forced to perform an approximate analysis with the existing relaxation models that do not allow for a precise quantitative evaluation of the measured parameters. We believe that this deficiency is at present a general feature of the existing NMR relaxation studies of QCs and cannot be overcome before a substantial theoretical progress on the electronic states in QCs is made.

VI. CONCLUSIONS

In the search for the sharp features in the electronic DOS of quasicrystals, a systematic comparative study of the DOS in the vicinity of E_F was performed on icosahedral $AlPdMn_{7.1}$, $AlCuFe_{12.5}$, and $AlPdRe_{8.5}$ by the ^{27}Al NMR spin-lattice relaxation. The investigated samples differ markedly in their electrical conductivity (and thus the DOS at E_F) and the content of paramagnetic centers. The paramagnetism introduces a strong relaxation mechanism of spin diffusion to paramagnetic centers that competes with the relaxation via conduction electrons and becomes dominant at low temperatures, typically below 100 K. The $AlPdMn_{7.1}$ and $AlCuFe_{12.5}$ show a parabolic variation of the pseudogap in the DOS, but no sharp features were detected. The reason for the lack of

observation of the sharp features could also be the masking of their effect by the strong paramagnetic relaxation. In the $AlPdRe_{8.5}$ the paramagnetic relaxation is absent except at temperatures below 7 K and a single sharp feature of the FWHH 14 meV, displaced by 11 meV from E_F, was clearly detected. The sharp feature is very deep, reducing the DOS at the minimum to a few percent of its value in the metallic aluminum. The shape of the DOS in the $AlPdRe_{8.5}$ reconstructed from the NMR parameters indicates that it may not be relevant to distinguish between the broad pseudogap and the sharp feature in this case. Instead, it seems more appropriate to consider the resulting shape as the global shape of the pseudogap that is deep, narrow and steep in the vicinity of E_F and becomes broader with a paraboliclike shape at distances a few ten meV away from the E_F. This shape of the pseudogap and the low DOS value at the minimum—as compared to the metallic aluminum as well as to the other two investigated QCs—can explain the much higher electrical resistivity of the *i*-AlPdRe family as compared to the *i*-AlCuFe and *i*-AlPdMn. The small displacement of the minimum in the DOS of the $AlPdRe_{8.5}$ from the exact E_F value can be viewed to arise naturally from the Hume-Rothery rules that predict the formation of the pseudogap exactly at E_F only for a sharp ''ideal'' composition of the alloy. Since the ideal composition is difficult to match in real samples, the displacement of the minimum in the DOS from E_F should appear more as a rule than as an exception in the experimental observations on real QCs.

ACKNOWLEDGMENT

S.J.P. acknowledges the support by the NSF Grant No. DMR97-00584.

[1] C. Janot and M. de Boissieu, Phys. Rev. Lett. **72**, 1674 (1994).
[2] T. Fujiwara and T. Yokokawa, Phys. Rev. Lett. **66**, 333 (1991).
[3] T. Fujiwara, S. Yamamoto, and G. Trambly de Laissardiere, Phys. Rev. Lett. **71**, 4166 (1993).
[4] T. Fujiwara, J. Non-Cryst. Solids **156/157**, 865 (1993).
[5] J. Hafner and M. Krajčí, Phys. Rev. Lett. **68**, 2321 (1992).
[6] M. Mori, S. Matsuo, T. Ishimasa, T. Matsuura, K. Kamiya, H. Inokuchi, and T. Matsukawa, J. Phys.: Condens. Matter **3**, 767 (1991).
[7] G. W. Zhang, Z. M. Stadnik, A. P. Tsai, and A. Inoue, Phys. Rev. B **50**, 6696 (1994).
[8] E. Belin, Z. Dankhazi, A. Sadoc, Y. Calvayrac, T. Klein, and J. M. Dubois, J. Phys.: Condens. Matter **4**, 4459 (1992).
[9] E. Belin and A. Traverse, J. Phys.: Condens. Matter **3**, 2157 (1991).
[10] R. Escudero, J. C. Lasjaunias, Y. Calvayrac, and M. Boudard, J. Phys.: Condens. Matter **11**, 383 (1999).
[11] X.-P. Tang, E. A. Hill, S. K. Wonnell, S. J. Poon, and Y. Wu, Phys. Rev. Lett. **79**, 1070 (1997).
[12] A. Shastri, D. B. Baker, M. S. Conradi, F. Borsa, and D. R. Torgeson, Phys. Rev. B **52**, 12 681 (1995).
[13] F. S. Pierce, S. J. Poon, and Q. Guo, Science **261**, 737 (1993).
[14] T. Apih, O. Plyushch, M. Klanjšek, and J. Dolinšek, Phys. Rev. B **60**, 14 695 (1999).
[15] J. Winter, *Magnetic Resonance in Metals* (Clarendon, Oxford, 1971), p. 42.
[16] J. C. Lasjaunias, A. Sulpice, N. Keller, and J. J. Préjean, Phys. Rev. B **52**, 886 (1995).
[17] M. A. Chernikov, A. Bernasconi, C. Beeli, A. Schilling, and H. R. Ott, Phys. Rev. B **48**, 3058 (1993).
[18] J. C. Lasjaunias, Y. Calvayrac, and Hongshun Yang, J. Phys. I **7**, 959 (1997).
[19] A. Abragam, *The Principles of Magnetic Resonance* (Oxford University Press, London, 1960), p. 378.
[20] J. Dolinšek, T. Apih, M. Simsič, and J. M. Dubois, Phys. Rev. Lett. **82**, 572 (1999).
[21] H. R. Ott (private communication).
[22] J. L. Gavilano, B. Ambrosini, P. Vonlanthen, M. A. Chernikov, and H. R. Ott, Phys. Rev. Lett. **79**, 3058 (1997).
[23] J. C. Lasjaunias, A. Sulpice, N. Keller, J. J. Préjean, and M. de Boissieu, Phys. Rev. B **52**, 886 (1995).